Available online at www.sciencedirect.com
SCIENCE DIRECT®

Journal of the European Ceramic Society 24 (2004) 699–703

www.elsevier.com/locate/jeurceramsoc

Mechanical properties of fibrous monolithic Si_3N_4/BN ceramics with different cell boundary thicknesses

Young-Hag Koh*, Hae-Won Kim, Hyoun-Ee Kim

School of Materials Science and Engineering, Seoul National University, Seoul, 151-742, South Korea

Received 3 February 2003; received in revised form 12 March 2003; accepted 15 March 2003

Abstract

Fibrous Si_3N_4/BN monoliths with various cell boundary thickness were fabricated by hot-pressing. The extruded Si_3N_4 polymer was dip-coated with the BN-containing slurry with a different BN concentration. A cell boundary thickness increase up to 42 μm by adjusting the BN concentration from 0 to 25 wt.% in the slurry, and this cell boundary thickness was found to play an important role in determining the fracture behavior of the fibrous monoliths. On increasing cell boundary thickness, the flexural strength decreased, but the apparent work-of-fracture and toughness increased remarkably due to the extensive crack interactions with weak cell boundaries. This is related to the change in stored energy before fracture initiation and in interfacial fracture resistance.

Keywords: BN; Composites; Si_3N_4; Strength; Toughness; Work-of-fracture

1. Introduction

Silicon nitride (Si_3N_4) is regarded as one of the most promising materials for high-temperature structural applications due to its excellent thermomechanical properties, such as high strength, hardness, and resistance to creep and oxidation at elevated temperatures. However, its wider utilization has been limited mainly because of its catastrophic fracture behavior. Many efforts have been made to prevent the catastrophic fracture pattern of ceramics,[1,2] including fiber reinforcement,[3] lamination,[4–10] and the production of fibrous ceramics.[11–21] Among those composites, fibrous monolithic ceramics consist of a primary phase (Si_3N_4 cell) and a tailored phase (BN cell boundary).[12] Non-catastrophic failures are frequently observed in fibrous monolithic materials because of crack interactions with the weak cell boundaries.[12–21] In other words, cracks propagate through the cell boundaries, which results in a high fracture energy requirement, as is the case of crack deflection or crack delamination.

Research on fibrous Si_3N_4/BN monoliths has been focused on finding the mechanism of crack deflection and delamination[4,12,22–24] and on the optimization of their mechanical properties through processing improvements.[12,25] Crack interactions are strongly dependent on the characteristics of both the cell and the cell boundaries, especially their relative elastic moduli, strengths, toughnesses, and thermal expansion coefficients.[12] Also, the cell boundary thickness is expected to play a key role in the fracture behavior of fibrous monoliths.

Therefore, in the present research, we investigated the effect of cell boundary thickness on mechanical properties, including strength, apparent work-of-fracture, and fracture toughness of fibrous monolithic Si_3N_4/BN composites. The thickness of the cell boundaries was controlled by changing the BN concentration in the slurry used for the dip-coating process.

2. Experimental procedures

A high purity α-Si_3N_4 powder (E-10, Ube Industries, Tokyo, Japan) was mixed with 5 wt.% yttria (Grade F, H. C. Starck GmbH & Co., Berlin, Germany) and 2

* Corresponding author. Now with University of Michigan.
E-mail address: younghag@engin.umich.edu (Y.-H. Koh).

0955-2219/03/$ - see front matter © 2003 Elsevier Ltd. All rights reserved.
doi:10.1016/S0955-2219(03)00266-8

wt.% alumina (HP-DBM, Reynolds, Bauxite, AK, USA) as sintering additives. It was then ball-milled in ethanol with silicon nitride balls as media for 24 h. After milling, the mixture was dried in a rotary vacuum evaporator and subsequently passed through a 60-mesh screen. The powder was mixed again with a polymer binder (methylcellulose), plasticizer (glycerol), and solvent (distilled water) at room-temperature for extrusion.

The cell boundary material was prepared by mixing the BN powder (Grade MBN, Boride Ceramics & Composites Ltd, UK) with 20 wt.% Al_2O_3 as a sintering aid. A polymer binder (PVB), dispersant (Menhaden fish oil), and solvent (trichloroethylene/ethanol) were also added, and mixed by ball milling for 6 h. The amount of BN-containing material increased up to 25 wt.% for different cell boundary thicknesses. The as-received BN powder showed platelets with a dimension of 1–10 μm and a thickness of 0.1–0.5 μm. The total oxygen content, including B_2O_3, was less than 5 wt.%. The cell was made by extruding the Si_3N_4-polymer compound into ~300 μm diameter fibers and was coated with BN by passing through the BN-containing slurry, and subsequently arrayed by an automatic winding machine. The layered green billets were cut into the desired dimension, and then dried in the oven at 80 °C for 12 h to improve the shape and strength of cell by hardening. The layered green billets were inserted into a mold of 40×40 mm and pressed at 0.5 MPa. Binder burnout of billets occurred in 900 °C with heating rate of 2–3 °C/min and maintained for 3 h in flowing nitrogen. Billets were hot-pressed at 1800 °C for 1 h under an applied load of 30 MPa in a flowing nitrogen atmosphere.

Specimens for mechanical testing were machined into a bar shape with dimensions of 3×4×25 mm and ground with a 800-grit diamond wheel. The tensile side of the specimens was polished with diamond slurries down to 1 μm, and then chamfered to minimize the machining flaws. The flexural strength was measured using a four-point flexural configuration with a crosshead speed of 0.05 mm/min, and inner- and outer-spans of 10 and 20 mm, respectively. From the load versus crosshead deflection response, the apparent work-of-fracture was calculated by estimating the area under the load-deflection curve and dividing by twice the cross-sectional area of the sample. Apparent fracture toughness was measured using the single-edge-notched beam (SENB) method. A straight notch with depth and width of 1.2 and 0.3 mm, respectively, was made at the center of the tensile surface using a thin diamond blade. The notched specimen was fractured using the four-point flexural configuration mentioned earlier. The density of the specimens was measured using the Archimedes method. The specimens were characterized by scanning electron microscopy (SEM), energy dispersive spectrometry (EDS), and X-ray diffraction (XRD).

3. Results and discussion

The typical microstructure of the Si_3N_4/BN fibrous monolith is shown in Fig. 1. Flat hexagonal Si_3N_4 cells were surrounded by continuous BN cell boundaries. According to the XRD analyses, the Si_3N_4 was completely transformed into the β-phase and no reaction occurred between the Si_3N_4 and the BN. However, EDS analyses showed that a glass phase (Si–Y–Al–N–O) was present at the cell boundaries as well as in the cells, implying that the glass phase migrated into the cell boundaries during the hot-pressing.

The thickness of the cell boundary layer was controlled by adjusting the BN concentration in the dip-coating slurry, and was measured by image analyses of SEM micrographs (see Fig. 1). The boundary layer thickness was found to be linearly dependent on the BN concentration as shown in Fig. 2. Therefore, fibrous monoliths with desired cell boundary thicknesses were fabricated simply by changing the BN concentration in the slurry. The specimen with 0 μm-cell boundary thickness represents the monolithic Si_3N_4.

The cell boundary thickness was found to have a strong influence on the fracture behavior of the fibrous materials. Representative stress versus deflection curves of the specimens with different cell boundary thicknesses are shown in Fig. 3. Monolithic Si_3N_4 exhibited typical catastrophic failure [Fig. 3(A)] as is frequently observed in other ceramics. However, the Si_3N_4 fibrous monolith with 18-μm thick BN cell boundary was not completely fractured even after reaching critical stress, as shown in Fig. 3(B). The gradual fractures became more profound with increased cell boundary thickness. When the cell boundary thickness reached 37 μm, the material was fractured in a non-brittle manner [Fig. 3 (C)], which implied active crack interactions at the cell boundaries.

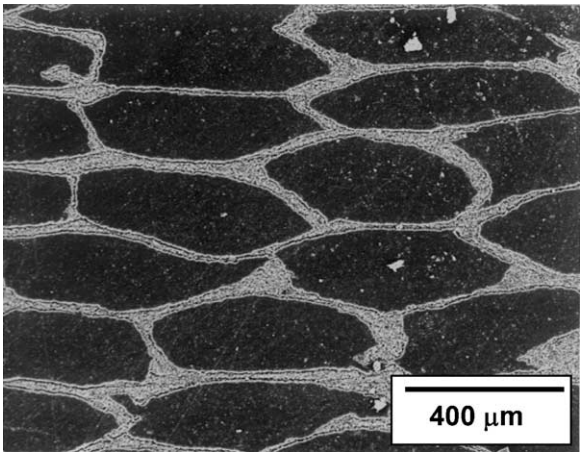

Fig. 1. A representative SEM micrograph of cross-section of a fibrous Si_3N_4/BN monolith.

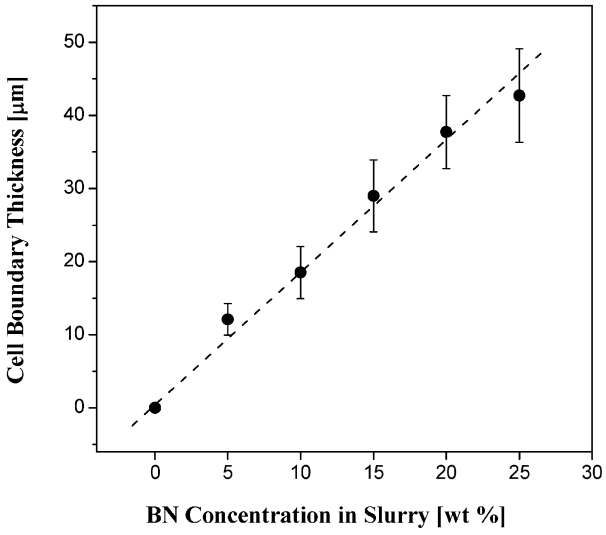

Fig. 2. Cell boundary thickness of the specimens as a function of BN concentration in the slurry.

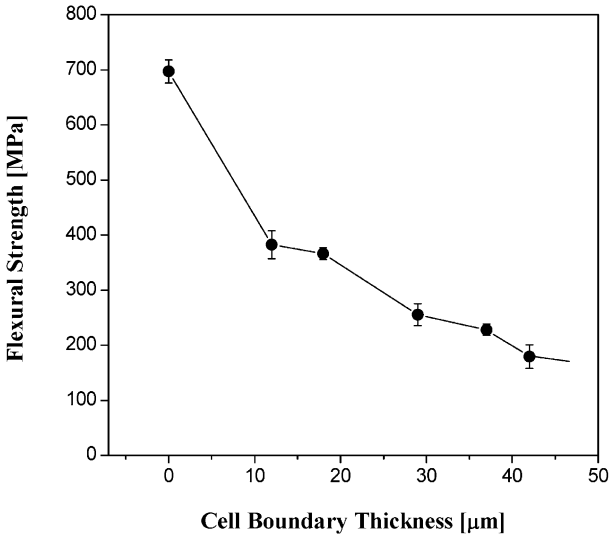

Fig. 4. Flexural strength of the specimens as a function of cell boundary thickness.

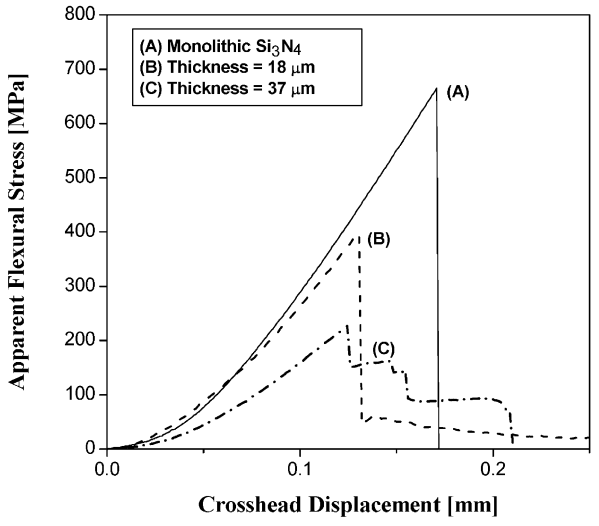

Fig. 3. Flexural response of specimens with cell boundary thicknesses of (A) 0, (B) 18, and (C) 37 μm.

The maximum stress recorded in Fig. 3 corresponds to the flexural strength of the material. The strength of fibrous monoliths with respect to the cell boundary thickness is shown in Fig. 4. As expected, the strength of fibrous monoliths was lower than that of monolithic Si_3N_4, and decreased steadily with increasing cell boundary thickness. This decrease in flexural strength was due to the increase in flaw size which might be present in cell boundaries. However, the strengths were not very sensitive to the boundary thickness except for 0-μm cell boundary thickness (i.e. monolithic Si_3N_4), presumably because the size of the critical flaws responsible for fracture was not strongly dependent on the cell boundary thickness.

For structural ceramic applications, energy dissipation capacity during fracture is one of the most important criteria. The energy dissipated by the sample during the non-catastrophic failure is estimated by the apparent work-of-fracture, which corresponds to the area under the load–deflection curve after the first load drop (inelastic region). Despite the decrease in strength, the work-of-fracture increased markedly for fibrous monoliths, as shown in Fig. 4. When the cell boundary was very thin (~10 μm), the specimen fractured in a brittle manner. However, with increasing the cell boundary thickness, the work-of-fracture also increased. Maximum work-of-fracture in the present research was observed for the specimen with a boundary thickness of 37 μm. When the cell boundary was thicker than this, the work-of-fracture decreased sharply, as shown in Fig. 5. These results suggest that the work-of-fracture is influenced by the strength of the material as well as by the crack propagation pattern. When the strength is too high, i.e. when too much strain energy is stored in the material, the crack propagates through the cells or cell boundaries without any significant crack interactions. On the other hand, when the strength is too low, the work-of-fracture is low because the material can withstand only limited stress.

The influence of cell boundary thickness on the crack pattern is demonstrated in the SEM micrographs, in Fig. 6. The fracture pattern of the fibrous monolithic specimen with boundary thickness of 18 μm is shown in Fig. 6(A). Unlike the monolithic materials, extensive crack deflections occurred at the cell boundaries. When the cell boundary thickness was increased to 37 μm, not only the crack deflections but also extensive crack delaminations occurred, as illustrated in Fig. 6(B). The improved work-of-fracture with increasing the cell

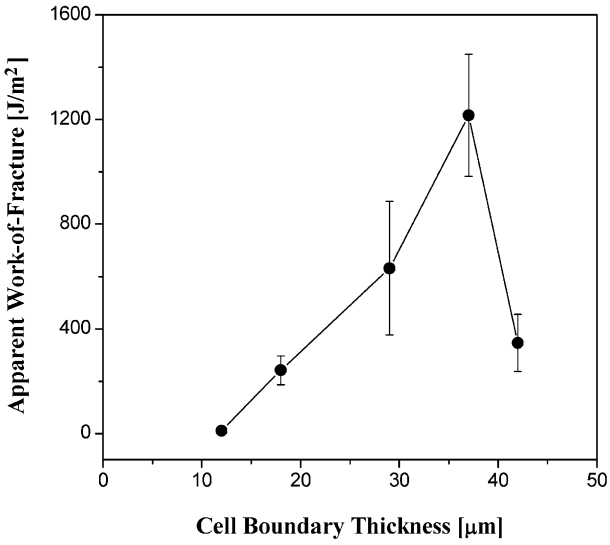

Fig. 5. Apparent work-of-fracture of the specimens as a function of cell boundary thickness.

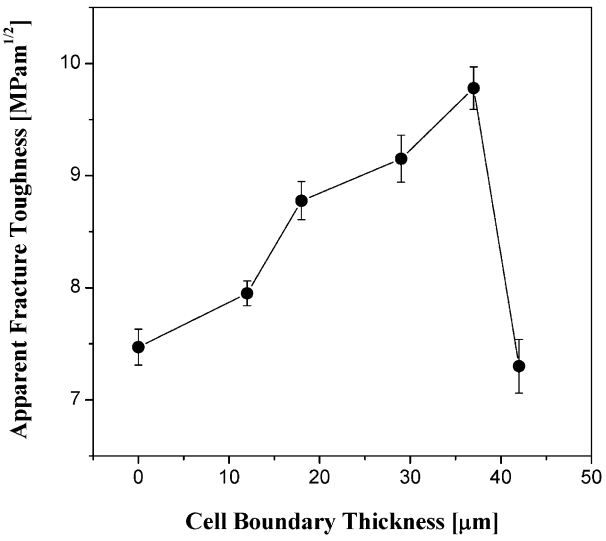

Fig. 7. Apparent fracture toughness of the specimens as a function of cell boundary thickness.

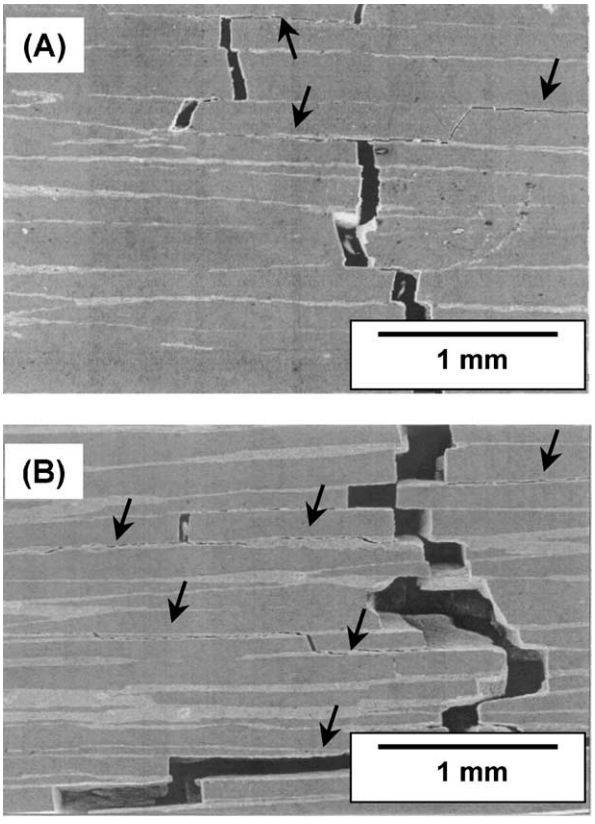

Fig. 6. SEM micrographs of crack propagations of the specimens with cell boundary thickness of (A) 18 and (B) 37 μm.

boundary thickness is attributed to these combined effects of crack deflections and delaminations.

Fracture toughness (Fracture toughness measurement by SENB method assumes elastic behaviour up to the load of failure. Therefore, the apparent fracture toughness for fibrous monolithus is reported as the "normal toughness" which the original intact specimen would have experienced at that load with a given notch depth.), which represents the material's resistance to the crack propagation, of the fibrous materials is shown in Fig. 7 as a function of cell boundary thickness, measured by the SENB method using a 1.2 mm crack depth. Monolithic Si_3N_4 is known to have a high fracture toughness (7.5 MPa $m^{1/2}$) due to the interactions between the cracks and elongated grains. Even though such elongated grains were not formed, the apparent fracture toughness of Si_3N_4 was enhanced by incorporating BN interlayers. Like the work-of-fracture, the apparent fracture toughness increased with cell boundary thickness until 37 μm (10 MPa $m^{1/2}$) and decreased thereafter. This improvement was again attributed to the crack interactions (i.e. crack deflections and delaminations) with the weak cell boundaries.

The advantage of the fibrous monolith is most clearly illustrated by the stress–deflection curve of the notched specimens. When the specimens had a notch on the surface, which corresponded to a surface crack, the fibrous monolith had a similar value of critical stress at failure as its monolithic counterpart (i.e. exhibits notch-insensitivity). Moreover, the fracture did not occur in a catastrophic fashion but in a stable manner, i.e. the load bearing capacity kept increasing after the first drop of stress.

The fracture behaviors of the fibrous monolith are strongly dependent on the properties of cell and cell boundary, such as elastic modulus, interfacial strength, surface flaw, and coefficient of thermal expansion (CTE).[12] Fibrous monoliths can show two possible fracture behaviors depending on the magnitude of crack interactions, that is, brittle and non-catastrophic failure. Considering the stored energy before fracture initiation, when the strength is too high, i.e. when too much strain

Table 1
Summarized mechanical properties of monolithic Si_3N_4 and fibrous monoliths with cell boundary thickness of 37 μm

Samples	MOR (MPa)	WOF (J/m^2)	K_{IC} (MPa $m^{1/2}$)
Monolithic Si_3N_4	697±21	Negligible	7.5±0.16
Fibrous monolith	227±11	1216±233	10±0.19

energy is stored in the material, the crack propagates through the cells and the cell boundaries without any significant crack interactions. On the other hand, when the strength is too low, the work-of-fracture is low because the material can withstand only limited stress (see Fig. 5). Fracture behavior is dependent on the stored energy before fracture initiation, as well as the change in interfacial fracture resistance by different cell boundary thickness. Therefore, cell boundary thickness is one of the most critical factors for obtaining high WOF. The mechanical properties of monolithic Si_3N_4 and fibrous monolith with cell boundary thickness of 37 μm are listed in Table 1. The WOF and facture toughness increased remarkably for fibrous monolith with non-catastrophic failure.

4. Conclusion

Fibrous monolithic ceramics consisting of strong Si_3N_4 cells surrounded by weak BN cell boundaries with various thicknesses were fabricated by hot-pressing. Si_3N_4-polymer was extruded, and then coated with a BN-containing slurry by dip-coating. Cell boundary thickness was controlled by adjusting the concentration of BN in the slurry. On increasing the cell boundary thickness, the density decreased and the fracture behavior changed from a brittle pattern to one of the non-catastrophic failure type. Mechanical properties of these fibrous monoliths were significantly affected by these distinctive fracture behaviors. When the cell boundary thickness was increased, the flexural strength decreased due to the reduction in the volume fraction of the Si_3N_4. However, the apparent work-of-fracture and the fracture toughness increased significantly due to the extensive crack interactions with the weak BN cell boundaries. These different fracture behaviors were related to the energy stored before fracture initiation and the change in the interfacial fracture resistance.

References

1. Harmer, M. P., Chan, H. M. and Miller, G. A., Unique opportunities for microstructural engineering with duplex and laminar ceramic composites. *J. Am. Ceram. Soc.*, 1992, **75**, 1715–1728.
2. Evans, A. G., Perspective on the development of high-toughness ceramics. *J. Am. Ceram. Soc.*, 1990, **73**, 187–206.
3. Kerans, R. J. and Parthasarathy, T. A., Crack deflection in ceramic composites and fiber coating design criteria. *Composites*, 1999, **A30**, 521–524.
4. Kovar, D., Thouless, M. D. and Halloran, J. H., Crack deflection and propagation in layered silicon nitride–boron nitride ceramics. *J. Am. Ceram. Soc.*, 1998, **81**, 1004–1012.
5. She, J., Inoue, T. and Ueno, K., Damage resistance and R-curve behavior of multilayer Al_2O_3/SiC ceramics. *Ceramic International*, 2000, **26**, 801–805.
6. Russo, C. J., Harmer, M. P., Chan, H. M. and Miller, G. A., Design of a laminated ceramic composite for improved strength and toughness. *J. Am. Ceram. Soc.*, 1992, **75**, 3396–3400.
7. She, J., Inoue, T. and Uneo, K., Multilayer Al_2O_3/SiC ceramics with improved mechanical behavior. *J. Eur. Ceram. Soc.*, 2000, **20**, 1771–1775.
8. Liu, H. and Hsu, S. M., Fracture behavior of multilayer silicon nitride/boron nitride ceramics. *J. Am. Ceram. Soc.*, 1996, **79**, 2452–2457.
9. Ohji, T., Shigegaki, Y., Miyajima, T. and Kanzaki, S., Fracture resistance behavior of multilayered silicon nitride. *J. Am. Ceram. Soc.*, 1997, **80**, 991–994.
10. Clegg, W. J., Kendall, X., Alford, K.McN., Button, T. W. and Birchall, J. D., A simple way to make tough ceramics. *Nature (London)*, 1990, **357**, 455–457.
11. Coblenz, W. S., *Fibrous Monolithic Ceramic and Method for Production*. US Patent, No. 4, 772524, 1998.
12. Kovar, D., King, B. H., Trice, R. W. and Halloran, J. H., Fibrous monolithic ceramics. *J. Am. Ceram. Soc.*, 1997, **80**, 2471–2487.
13. Baskaran, S., Nunn, S. D., Popovic, D. and Halloran, J. H., Fibrous monolithic ceramics: I, fabrication, microstructure, and indentation behavior. *J. Am. Ceram. Soc.*, 1993, **76**, 2209–2216.
14. Baskaran, S. and Halloran, J. H., Fibrous monolithic ceramics: II, flexural strength and fracture behavior of the silicon carbide/graphite system. *J. Am. Ceram. Soc.*, 1993, **76**, 2217–2224.
15. Baskaran, S. and Halloran, J. H., Fibrous monolithic ceramics: III, mechanical properties and oxidation behavior of the silicon carbide/boron nitride system. *J. Am. Ceram. Soc.*, 1994, **77**, 1249–1255.
16. Baskaran, S., Nunn, S. D. and Halloran, J. H., Fibrous monolithic ceramics: IV, mechanical properties and oxidation behavior of the alumina/nickel system. *J. Am. Ceram. Soc.*, 1994, **77**, 1256–1262.
17. Trice, R. W. and Halloran, J. H., Influence of microstructure and temperature on the interfacial fracture energy of silicon nitride/boron nitride fibrous monolithic ceramics. *J. Am. Ceram. Soc.*, 1999, **82**, 2502–2508.
18. Trice, R. W. and Halloran, J. H., Elevated-temperature mechanical properties of silicon nitride/boron nitride fibrous monolithic ceramics. *J. Am. Ceram. Soc.*, 2000, **83**, 311–316.
19. Trice, R. W. and Halloran, J. H., Effect of sintering aid composition on the processing of Si_3N_4/BN fibrous monolithic ceramics. *J. Am. Ceram. Soc.*, 1999, **82**, 2943–2947.
20. Hai, G., Yong, H. and An, W. C., Preparation and properties of fibrous monolithic ceramics by in-situ synthesizing. *J. Mater. Sci.*, 1999, **34**, 2455–2459.
21. She, J., Inoue, T., Suzuki, M., Sodeoka, S. and Ueno, K., Mechanical properties and fracture behavior of fibrous Al_2O_3/SiC ceramics. *J. Eur. Ceram. Soc.*, 2000, **20**, 1877–1881.
22. Folsom, C. A., Zok, F. W. and Lange, F. F., Flexural properties of brittle multilayer materials: I, modeling. *J. Am. Ceram. Soc.*, 1994, **77**, 689–696.
23. He, M.-Y. and Hutchinson, J. W., Crack deflection at an interface between dissimilar elastic materials. *Int. J. Solids. Struct.*, 1989, **l25**, 1053–1067.
24. Camus, G., Modeling of the Mechanical behavior and damage process of fibrous ceramic matrix composites: application to a 2-D SiC/SiC. *Int. J. Solids. Struct*, 2000, **37**, 919–942.
25. King, B. H., Influcence of Architecture on the Mechnaical Properties of Fibrous Monolithic Ceramics. PhD Thesis, University of Michigan, Ann Arbor, MI, 1997.